Nanoscience and
Nanotechnology Letters
Vol. 6, 68–71, 2014

Rice Husk-Derived Activated Carbon for Li Ion Battery Anode

Xiang Peng[1], Jijiang Fu[1, 2 *], Chengcheng Zhang[1], Jingyuan Tao[1], Lan Sun[1], and Paul K. Chu[2 *]

[1]School of Material and Metallurgy, Wuhan University of Science and Technology, Wuhan 430081, China
[2]Department of Physics and Materials Science, City University of Hong Kong, Kowloon, Hong Kong, China

Chemically activated carbon extracted from rice husks is used as anode materials in lithium ion batteries. The synthesized porous carbon exhibits a low degree of graphitization and nanoporous microstructure. The activated carbon anode possesses excellent charge/discharge properties at a current density of 0.2 C and the reversible specific capacitance is 730 mA h g^{-1} in the first cycle. The coulombic efficiency is maintained at 99% after 3 cycles and the capacitance remains at 400 mA h g^{-1} after 60 cycles.

Keywords: Rice Husk, Chemical Activated, Activated Carbon, Lithium Ion Battery, Biomass.

1. INTRODUCTION

Carbon materials are ideal candidates in energy storage and conversion applications. They can be used as electrode materials in Li-ion batteries (LIB) and supercapacitors, catalysts for the oxygen reduction in fuel cells, and host materials for hydrogen storage.[1–4] Synthesis of carbon materials typically consumes fossil resources which are severely diminishing and hence, a renewable energy source should be considered when producing carbon materials in order to minimize environmental impact.

Biomasses are recyclable and abundant on earth and their conversion into usable carbon is a green and economical method. Up to date, porous active carbon has been derived from a serious of natural biomasses such as cassava peel waste, chicken eggshell, seed shell, rubber wood sawdust, wood, peanut kernel, and sugar,[5–8] of which rice husks (RH) as a common form of agricultural biomass is a major by-product produced by the rice milling industry. The global rice production is about 600 million tons per year and there are more than 100 million tons of RH (RH makes up about 20% of the rice paddy weight). The overall carbon content in RH is more than 37% by weight (as shown in Table I).[9–12] It is therefore of both technological and commercial interest to produce activated carbon from RH. Activated carbon has been fabricated from RH by reacting with alkali hydroxides (KOH and NaOH) at a relatively high temperature and used in supercapacitors and adsorption ability.[13, 14] The common anode materials in commercial LIB are graphite (with the theoretical capacity of 372 mA h g^{-1})[15] and one promising utilization of RH is the generation of sustainable carbon materials for LIB anodes.

In this letter, amorphous nanoporous activated carbon is produced from RH by first HCl etching, subsequent thermal carbonization under argon at 550 °C for 4 h and alkali hydroxide activation at 800 °C for 1 h. The specific capacity of the activated carbon reaches 730 mA h g^{-1} in the initial charge/discharge process at a current density of 0.2 C (~ 75 mA g^{-1}) and remains at 140 mA h g^{-1} at 10 C (~ 3.75 A g^{-1}). After 3 cycles, the coulombic efficiency is above 99% and the capacity remains at ~ 400 mA h g^{-1} after charging/discharging for 60 cycles. The high capacity, rate capacity, and long-term cycle life of the activated carbon prepared from RH suggest promising applications to LIB anode electrodes.

2. EXPERIMENTAL DETAILS

RH obtained from a local rice mill was washed thoroughly with distilled water to remove soil and then boiled in HCl (2 mol L^{-1}) for 2 h to get rid of metallic oxides. The RH was then annealed in a tube furnace at 550 °C for 4 h under Ar to remove small organic molecules. Afterwards, the pre-carbonized carbon was mixed with KOH at a weight ratio of 4:1 and further heated to 800 °C for 1 h under N_2 to form nanoporous mocrostructure. The product was washed with water for several times and then dried at 100 °C to produce the activated carbon (black powders).

The samples were characterized by X-ray diffraction (XRD, Philips X'Pert Pro) with Cu K_a radiation

*Authors to whom correspondence should be addressed.

 1941-4900/2014/6/068/071 doi:10.1166/nnl.2013.1714

Table I. Proximate analysis of rice husk.

Proximate analysis (wt%)	
lignin	22
cellulose	38
hemicelluloses	18
silica	20
metal oxides	2
Metal content (wt%)	
K_2O	0.60
Na_2O	0.42
CaO	0.38
MgO	0.47
Fe_2O_3	0.13

(wavelength of 0.15416 nm) in the range of 10~90° (2θ) and micro-Raman scattering (Renishaw 2000 Raman spectrometer equipped with a 514.5 nm Ar laser) was conducted at room temperature. The specific surface area on the sample was determined by the Brunauer-Emmett-Teller (BET) method using an automated chemisorption/physisorption surface area analyzer (Micromeritics ASAP 2020) at 77 K.

The electrode was prepared by mixing the as-prepared active carbon (80 wt%), carbon black (10 wt%), and polyvinylidene fluoride (PVDF, 10 wt%) in N-methylpyrrolidone (NMP) to form a homogenous slurry. The slurry was coated on a Cu foil and dried at 120 °C overnight in a vacuum oven. 1 M $LiPF_6$ in a mixture of ethylene carbonate (EC) and dimethyl carbonate (DMC) (1:1 by volume) served as the electrolyte. Assembly of the test cells was carried out in an argon-filled glove box. The batteries were charged/discharged at different rates from 0.2 C to 10 C between 0 and 3.0 V (vs. Li/Li^+) on a LAND CT2001A cell test apparatus (1 C corresponding to 372 mA g^{-1}).

3. RESULTS AND DISCUSSION

The elemental composition of the as-prepared black products is determined by XRD and Raman scattering. The XRD spectrum in Figure 1(a) shows a broad (002) peak

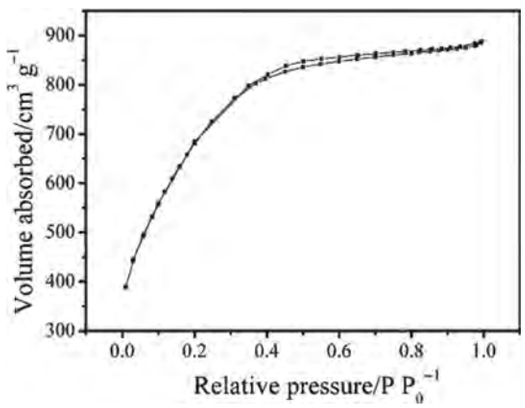

Fig. 2. Adsorption and desorption isotherms of N_2 measured at 77 K from the activated carbon.

at 25° indicative of the disordered nature. The weak (100) peak at 43° suggests small islands of coherent and parallel stacked graphene sheets. In the Raman scattering spectrum in Figure 1(b), the two obvious peaks at 1350 and 1600 cm^{-1} correspond to the D and G bands of amorphous carbon, respectively.[16] Based on the characterization results, amorphous activated carbon is produced from RH.

To investigate the specific surface area and microstructure of the RH derived carbon products, the BET adsorption and desorption isotherms of N_2 are acquired at 77 K. As shown in Figure 2, the activated carbon displays a type I desorption isotherm. The amount of adsorbed N_2 increases rapidly until a pressure of 0.4 and then more slowly after the relative pressure reaches 0.4 and high due to capillary condensation induced by the nanoporous holes. The as-prepared RH carbon has a microporous structure and the specific surface area and average pore size are ~ 2,500 m^2 g^{-1} and 2.2 nm, respectively, which are suitable for Li^+ suggesting potential applications as high performance electrodes in lithium batteries. To investigate the resistance of the RH derived activated carbon, electrochemical impedance spectroscopy (EIS) is performed after 3 cycles at a scanning rate of 0.2 mV s^{-1}. The Nyquist plot obtained from the activated carbon electrode

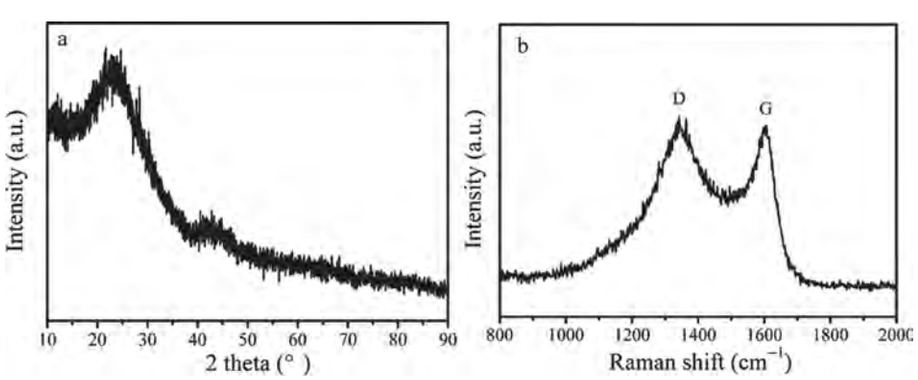

Fig. 1. XRD and Raman scattering spectra of the activated carbon.

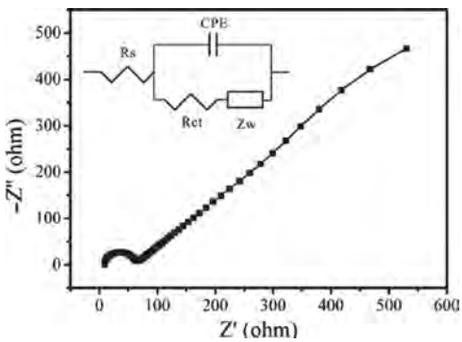

Fig. 3. EIS plot and equivalent circuit of the cell assembled with the activated carbon.

exhibits a depressed semicircle at high frequencies and an inclined line at low frequencies (Fig. 3). In general, the high-frequency semicircle is due to the combined effects of the contact, SEI resistance R_s, and charge transfer resistance R_{ct}.[17] The inclined line with an angle of approximately 45° to the real axis is attributed to the lithium-diffusion process in the carbon electrode. By simulating the kinetic parameters based on the typical Randles equivalent circuit,[18, 19] the values of R_s and R_{ct} for the RH activated carbon electrode are derived to be 8.6 ohm and 52 ohm, respectively, which are comparable with those of the GNS/CNF,[8] HGCNs,[20] and carbon coated SFG,[21] indicating high electrochemical activity of the activated carbon.

The activated carbon derived from the rice husk is evaluated as the anode in lithium ion batteries. The CV curves of the first three cycles at scanning rate of 0.2 mV s^{-1} are displayed in Figure 4(a). There are obvious reduction peaks in the potential range of 0.2–0.5 V and 0.7–1.0 V in the first cycle, which correspond to the irreversible reactions between the activated carbon electrode and electrolyte. The difference between the first cycle and second cycle is due to the incomplete conversion reaction and irreversible lithium loss as a result of the formation of the SEI film.[19, 22, 23] Between the second and third cycle, there is no obvious change implying that the electrode is stable after the first cycle. Figure 4(b) shows the charge/discharge curves of the first 10 cycles at a current density of 0.2 C (1 C corresponding to 372 mA g^{-1}). At this current density, the first charge capacity is as high as 730 mA h g^{-1}. As shown in Figure 4(c), the charge capacity decreases during the first few cycles but then stabilizes after about 10 cycles to ~400 mA h g^{-1}, which is higher than that of graphite (<372 mA h g^{-1}). The improvement can be attributed to the existence of many micropores in the activated carbon acting as reservoirs for lithium storage.[24] A large irreversible capacity is observed from the first discharge/charge process. However, after the initial 3 cycles, the coulombic efficiency is above 99%. The irreversible capacity is a common phenomenon in carbon-based electrodes in LIB. It stems from reduction of the electrolyte resulting in the formation of a solid electrolyte interphase (SEI) on

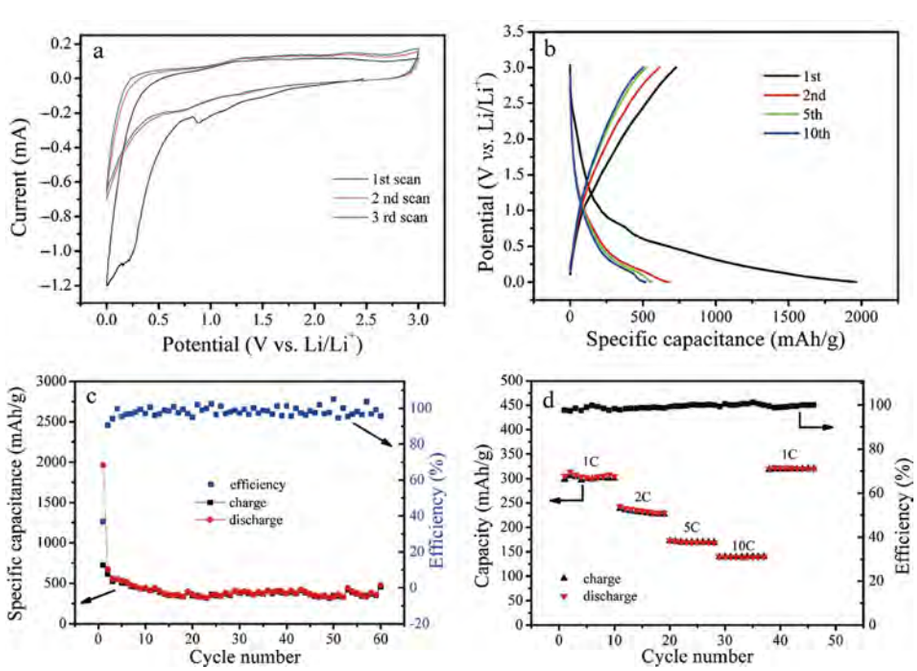

Fig. 4. Electrochemical performance of carbon derived from rice husk: (a) CV curves of the activated carbon in $LiPF_6$ with Li as the counter and reference electrodes, respectively, at a scanning rate of 0.2 mV s^{-1}; (b) Charge/discharge curves of the first 10 cycles at a current density of 0.2 C; (c) Capacity retention and coulombic efficiency behavior versus cycle number; (d) Rate performance at 1 C, 2 C, 5 C, 10 C, and then reverting back to 1 C.

the relatively large specific surface area of the sample (~ 2500 $m^2 g^{-1}$) and from irreversible lithium insertion into special positions because of the highly disordered carbon structure such as that in the vicinity of residual H atoms in the carbon materials.[14, 22, 25–28] To evaluate the rate performance, the cell is charged/discharged directly at various current densities for 10 cycles (Fig. 4(d)). The reversible capacities are 300, 240, 170, and 140 mA h g^{-1} at 1 C (0.375 A g^{-1}), 2 C (0.75 A g^{-1}), 5 C (1.875 A g^{-1}), and 10 C (3.75 A g^{-1}), respectively. When the rate is set back to 1 C (0.375 A g^{-1}) and after cycling at different current rates, the capacity can be recovered to 320 mA h g^{-1}. This rate performance of carbon material derived from biomasses is excellent.

4. CONCLUSION

Amorphous activated carbon is produced by pre-carbonization of rice husks (RH) at 550 °C for 4 h following by thermal activation at 800 °C for 1 h. The capacity of the activated carbon is as high as 730 mA h g^{-1} in the first charging/discharging process (~75 mA g^{-1}). It becomes stable after about 10 cycles and remains at 400 mA h g^{-1} after charging/discharging for 60 cycles. The coulombic efficiency is over 99% after the initial 3 cycles. The RH derived carbon electrode has a high rate capacity of 140 mA h g^{-1} at 10 C (~3.75 A g^{-1}). The high capacity, rate capacity, and long-term cycle life of the activated carbon produced from RH suggest promising applications to LIB anode electrodes.

Acknowledgments: This work was financially supported by National Natural Science Foundation of China (Grant Nos. 50902104 and 21105077), Hong Kong Research Grants Council (RGC) No. 112212, and City University of Hong Kong Applied Research Grants (ARG) Nos. 9667066 and 9667069.

References and Notes

1. B. J. Landi, M. J. Ganter, C. D. Cress, R. A. DiLeo, and R. P. Raffaelle, *Energy and Environmental Science* 2, 638 **(2009)**.
2. P. Simon and Y. Gogotsi, *Nat. Mater.* 7, 845 **(2008)**.
3. D. Cao, Y. Sun, and G. Wang, *J. Power Sources* 167, 250 **(2007)**.
4. A. C. Dillon, K. M. Jones, T. A. Bekkedahl, C. H. Kiang, D. S. Bethune, and M. J. Heben, *Nature* 386, 377 **(1997)**.
5. A. E. Ismanto, S. Wang, F. E. Soetaredjo, and S. Ismadji, *Bioresour. Technol.* 101, 3534 **(2010)**.
6. Z. Li, L. Zhang, B. S. Amirkhiz, X. Tan, Z. Xu, H. Wang, B. C. Olsen, C. M. B. Holt, and D. Mitlin, *Adv. Energy Mater.* 2, 431 **(2012)**.
7. A. Elmouwahidi, Z. Zapata-Benabithe, F. Carrasco-Marin, and C. Moreno-Castilla, *Bioresour. Technol.* 111, 185 **(2012)**.
8. M. Olivares-Marín, J. A. Fernández, M. J. Lázaro, C. Fernández-González, A. Macías-García, V. Gómez-Serrano, F. Stoeckli, and T. A. Centeno, *Mater. Chem. Phys.* 114, 323 **(2009)**.
9. A. Salanti, L. Zoia, M. Orlandi, F. Zanini, and G. Elegir, *J. Agr. Food Chem.* 58, 10049 **(2010)**.
10. M. Fang, L. Yang, G. Chen, Z. Shi, Z. Luo, and K. Cen, *Fuel Process. Technol.* 85, 1273 **(2004)**.
11. L. Armesto, A. Bahillo, K. Veijonen, A. Cabanillas, and J. Otero, *Biomass Bioenergy* 23, 171 **(2002)**.
12. L. Sun and K. Gong, *Ind. Eng. Chem. Res.* 40, 5861 **(2001)**.
13. Y. Guo, S. Yang, K. Yu, J. Zhao, Z. Wang, and H. Xu, *Mater. Chem. Phys.* 74, 320 **(2002)**.
14. H. Chen, H. Wang, L. Yang, Y. Xiao, M. Zheng, Y. Liu, and H. Fu, *Int. J. Electrochem. Sci.* 7, 4889 **(2012)**.
15. F. Bonino, P. R. S. Brutti1, L. G. B. Scrosati, J. Wu, and K. Müllen, *Adv. Mater.* 17, 743 **(2005)**.
16. X. Zhang, K. Huo, X. Peng, R. Xu, P. Li, R. Chen, G. Zheng, Z. Wu, and P. K. Chu, *Chem. Commun.* DOI: 10.1039/c3cc42583e,
17. S. Yang, H. Song, and X. Chen, *Electrochem. Commun.* 8, 137 **(2006)**.
18. S. Zhang and P. Shi, *Electrochim. Acta* 49, 1475 **(2004)**.
19. Y. Chen, Z. Lu, L. Zhou, Y. W. Mai, and H. Huang, *Nanoscale* 4, 6800 **(2012)**.
20. J. M. Tarascon and M. Armand, *Nature* 414, 359 **(2001)**.
21. Y.-S. Han and J.-Y. Lee, *Electrochim. Acta* 48, 1073 **(2003)**.
22. Z.-J. Fan, J. Yan, T. Wei, G.-Q. Ning, L.-J. Zhi, J.-C. Liu, D.-X. Cao, G.-L. Wang, and F. Wei, *ACS Nano* 5, 2787 **(2011)**.
23. Y.-K. Choi, K.-I. Chung, W.-S. Kim, and Y.-E. Sung, *Microchem. J.* 68, 61 **(2001)**.
24. F. Zhang, K. X. Wang, G. D. Li, and J. S. Chen, *Electrochem. Commun.* 11, 130 **(2009)**.
25. T. Takamura, H. Awano, T. Ura, and K. Sumiya, *J. Power Sources* 68, 114 **(1997)**.
26. Z. Wang, X. Huang, R. Xue, and L. Chen, *Carbon* 37, 685 **(1999)**.
27. M. Winter, J. O. Besenhard, M. E. Spahr, and P. Novμk, *Adv. Mater.* 10, 725 **(1998)**.
28. Y. S. Hu, P. Adelhelm, B. M. Smarsly, S. Hore, M. Antonietti, and J. Maier, *Adv. Funct. Mater.* 17, 1873 **(2007)**.

Received: 5 July 2013. Accepted: 13 August, 2013.